Research Square

Preprints are preliminary reports that have not undergone peer review.
They should not be considered conclusive, used to inform clinical practice,
or referenced by the media as validated information.

The Effects of Rainwater Infiltration on the Stability of the Khalid Djido Embankment Dam, Central Ethiopia Region, Ethiopia

Wondisha Mersha Taddese

coolwondi2023@gmail.com

Arba Minch University

Bogale GebreMariam Neka

Arba Minch University

Abebe Temesgen Ayalew

Arba Minch University

Research Article

Keywords: Rainwater infiltration, dam stability, pore pressure, finite element analysis, Khalid Djido embankment dam, PLAXIS 2D, SCS Curve Number

Posted Date: July 21st, 2026

DOI: https://doi.org/10.21203/rs.3.rs-8800796/v1

License: This work is licensed under a Creative Commons Attribution 4.0 International License.
Read Full License

Additional Declarations: No competing interests reported.

The Effects of Rainwater Infiltration on the Stability of the Khalid Djido Embankment Dam, Central Ethiopia.

Wondisha Mersha Taddese [1], Bogale GebreMariam Neka[2], Abebe Temesgen Ayalew[3]

[1,2,3.] Water Technology Institute, Arba Minch University, P.O. Box. 21, Arba Minch, Ethiopia

Corresponding Author: Wondisha Mersha Taddese; coolwondi2023@gmail.com

Abstract

Dam failure can cause severe flooding, property damage, and environmental degradation, making robust safety evaluation essential for embankment dams. This study assessed the effects of rainwater infiltration on the stability of the Khalid Djido embankment dam in Central Ethiopia. Coupled stress–pore water pressure analyses were conducted using PLAXIS 2D to directly link hydrological inputs with geotechnical responses under varying rainfall scenarios. Infiltration rates were estimated using the Soil Conservation Service (SCS) Curve Number method, while a regional Intensity–Duration–Frequency (IDF) analysis provided representative 24-hour rainfall intensity. Results revealed dynamic variations in pore water pressure, with maximum and minimum values of 34.07 kN/m² and –381.8 kN/m², respectively, highlighting critical instability zones. Significant pore pressure build-up was observed at the downstream toe during rainfall events. The factor of safety against slope failure ranged from 1.1 to 1.51, with lower values consistently associated with extreme rainfall, underscoring susceptibility to instability. These findings emphasize the importance of incorporating time-dependent infiltration effects in dam stability analyses, particularly in regions exposed to intense rainfall and hydro-climatic extremes. While the study provides valuable insights into infiltration-induced instability, it is limited by reliance on regional rainfall data, simplified soil parameter assumptions, and the absence of calibration against field monitoring data. Accordingly, all quantitative results should be interpreted with caution until site-specific validation becomes available.

Keywords: Rainwater infiltration, dam stability, pore pressure, finite element analysis, Khalid Djido embankment dam, PLAXIS 2D, SCS Curve Number

1. Introduction

Embankment dams play a crucial role in water resource management, providing essential services such as water storage for irrigation, drinking water supply, hydropower generation, and flood control [1]. However, the failure of these structures can lead to catastrophic

consequences, including loss of life, extensive property damage, environmental degradation, and severe economic disruption [2]. Therefore, ensuring the safety and stability of embankment dams is of paramount importance throughout their lifecycle. One of the significant factors affecting the stability of embankment dams, particularly in regions characterized by seasonal or intense rainfall, is rainwater infiltration [3]. The infiltration of rainwater into the dam body can induce dynamic changes in pore water pressure, significantly reduce soil shear strength, and ultimately compromise the structural integrity of the dam [4, 5, 6]. Understanding and accurately predicting the transient effects of rainwater infiltration on dam stability is thus crucial for effective dam design, operation, and maintenance.

In the context of Ethiopia, where many regions experience distinct wet and dry seasons with recurrent intense rainfall events, the risk of dam instability due to rainwater infiltration is particularly relevant [7]. Despite this critical regional context, comprehensive studies focusing on the integrated analysis of hydrological and geotechnical aspects of dam stability for specific, operational dams in Ethiopia, particularly with detailed transient rainfall characteristics, remain limited. This study aims to address this critical gap by investigating the effects of rainwater infiltration on the stability of the Khalid Djido embankment dam in the Central Ethiopia Region.

This research presents, to the best of the authors' knowledge, the first comprehensive study of the Khalid Djido dam, providing new insights into its behaviour under rainfall conditions. While the hydrological and geotechnical methods applied such as the SCS Curve Number (CN) method, Intensity-Duration-Frequency (IDF) analysis, and coupled stress–pore water pressure simulations in PLAXIS 2D are established approaches, their integrated application to this specific dam and regional hydro-climatic context represents a novel contribution. The study highlights the importance of explicitly modelling transient infiltration effects in Ethiopian embankment dams, where intense rainfall and seasonal variability pose significant stability challenges. While the general concept of integrating hydrological and geotechnical analyses is fundamental in dam safety assessment, the novelty of this study stems from this specific and detailed coupling of methods to explicitly model the transient response of an unstudied dam in a climatically sensitive Ethiopian context. This integrated approach allows for a more realistic and time-dependent assessment of dam behaviour under the dynamic influence of rainwater infiltration. Furthermore, the findings of this study provide new, invaluable insights into dam behaviour and the potential risks associated with rainwater infiltration in regions with similar

climatic conditions, contributing significantly to dam safety management practices and future design considerations.

2. Materials and Methods

2.1 Description of the Study Area

The Khalid Djido Embankment Dam is located in the Silti Zone of the Central Ethiopia region, approximately 175 km south of Addis Ababa. The catchment area includes parts of Alicho Woriro, Welbareg, Silte, and Dalocha Woredas. The dam's coordinates are 7° 49′ 38.55″ N, 38° 13′ 4.8″ E, at an elevation of 1,969 meters above sea level (masl). The region has a tropical climate with high rainfall and temperature variability and is prone to droughts, floods, landslides, and soil erosion. The tributaries drain into the Rift Valley Basin. Key rivers include the Djido, Furfuro, and Limaza. The Djido River drains into Lake Shalla and then the Rift Valley Basin at 1,519 masl. The catchment area covers 250.79 square kilometers. The topography significantly influences the region's climate, hydrology, soil, vegetation, agriculture, and human activities (Figure 1).

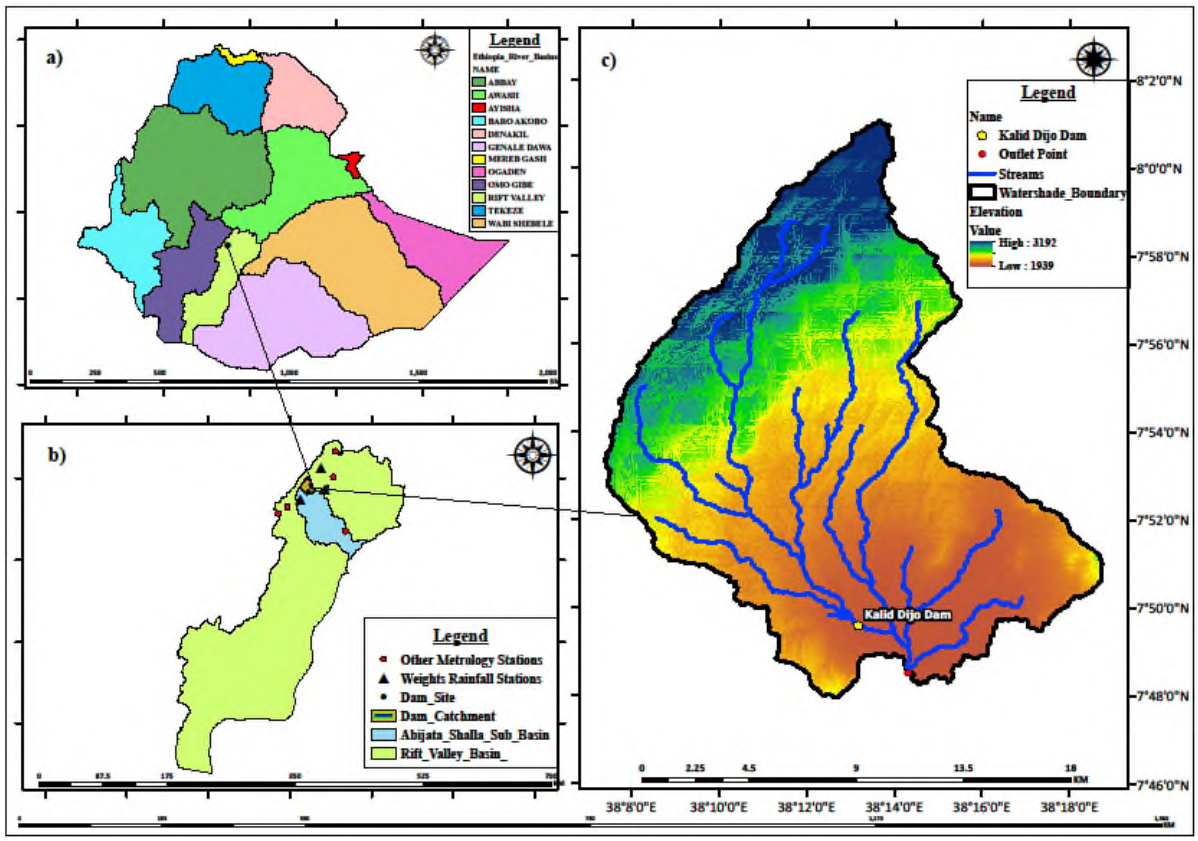


Fig. 1. Study area: a) Map of Ethiopia; b) Rift Valley Basin; c) Watershed

2.2 Hydrological Data and Analysis

2.2.1 Climate Data

Daily rainfall data from eight meteorological stations (Table 1) near the study area were collected. The data spanned from 1990 to 2021 and were obtained from the Ethiopian Meteorological Institute (EMI).

Table 1 Rainfall Stations near the Study Area

I.N	Station Name	Location GNS System		Altitude	Period of Record		% Missing
		Latitude	Longitude		Start	End	
1	**Arsinegele**	7° 21' 15.77" N	38° 40' 46.56" E	1952	1990	2021	12.09%
2	**Buie**	8° 19' 51.3" N	38° 33' 16.4" E	2053	1990	2021	4.32%
3	**Butajira**	8° 07' 21.4" N	38° 22' 33.4" E	2077	1990	2021	9.24%
4	**Fonko**	7° 38' 54.0" N	37° 58' 08.9" E	2244	1990	2021	3.99%
5	**Hossana**	7° 34' 04.1" N	37° 51' 22.1" E	2311	1990	2021	5.66%
6	**Koshe**	8° 0' 49.86" N	38° 31' 55.23" E	1871	1990	2021	1.87%
7	**Tora**	7° 51' 35.3" N	38° 25' 24.3" E	2011	1990	2021	5.79%
8	**Wulbareg**	7° 44' 17.9" N	38° 07' 22.0" E	1995	1990	2021	2.54%

2.2.2 Data Processing

Missing Precipitation Data: Missing rainfall data were estimated using the inverse distance method (IDM).

Consistency and Homogeneity: The consistency of the rainfall data was checked using the Double Mass Curve analysis and the homogeneity was assessed using the Rainfall Homogeneity Test. Homogeneity was achieved by adjusting inconsistent data points.

Rainfall Intensity-Duration-Frequency (IDF) Curves: IDF curves were derived from the rainfall data to characterize rainfall intensity for different durations and return periods.

2.2.3 Infiltration Rate Analysis

Infiltration rates were estimated using the Soil Conservation Service (SCS) Curve Number (CN) method. This empirical method relates cumulative rainfall to direct runoff volume based on soil type, land use, and antecedent moisture. The SCS-CN method is based on several key assumptions, including uniform land use and soil conditions, constant rainfall intensity, and a fixed initial abstraction (Equation 1, 2, 3 and 4) [8].

$$R = \frac{(I - I_A)^2}{(I + I_A) + S} \quad (1)$$

Where: S is the maximum volume storage in inches, I_A is the portion of S that is already occupied, and it is expressed as a fraction of S (typically 0.2). A common approach is to reduce the value of I_A, thus relaxing constraint that:

$$I_A = 0.2S \quad (2)$$

Values of S′ can be determined by the following empirical expression:

$$S = \frac{1000}{CN} - 10 \quad (3)$$

Where: CN is the soil curve number, S is in mm. For CN = 100, the storage capacity is zero, and the volume of runoff is equal to the cumulative infiltration. Therefore, the value of infiltration can be calculated by:

$$f = I - R \quad (4)$$

While practical for initial assessments, these assumptions can limit the method's accuracy, particularly in complex hydrological systems. In the case of a zoned embankment dam with clay core, filter layers, and permeable shell materials, the SCS-CN method's assumption of uniform soil conditions does not hold. The reported infiltration rate of 3.12 mm/hr. is an areal average that masks spatial variability, and more advanced infiltration models may yield different results. The SCS-CN method was applied to the study area, considering the predominant land use (agricultural fields, grasslands, and scattered settlements) and available soil data to determine appropriate CN values. It is essential to acknowledge the limitations of this method and consider potential uncertainties in the results.

2.3 Geotechnical Data

2.3.1 Soil type

Three dominant soil reference groups characterize the Khalid Djido Dam project area: deep Luvisols (49.4%), Vertisols (44.2%), and Cambisols (6.4%). These soils primarily consist of clay/clay loam (over 88%) and exhibit drainage varying from well drained to moderately drained, with some imperfections. Their sub-angular blocky structure, combined with a high available water content (AWC), makes them suitable for irrigation.

Soil Classification Methodology

The classification of soils at the Khalid Djido Dam site was based on a combination of field surveys and laboratory analyses. Field investigations included borehole drilling, in-situ density tests, and visual soil profiling, while laboratory tests comprised grain size distribution, Atterberg limits, and triaxial shear strength analyses. These results were used to identify soil texture, plasticity, and drainage characteristics. The classification system adopted was the FAO/World Reference Base (WRB) for Soil Resources, which is widely applied in Ethiopia

for engineering and agricultural studies. Within this framework, the soils were categorized as deep Luvisols (49.4%), Vertisols (44.2%), and Cambisols (6.4%). The classification was cross-checked against Ethiopian soil survey standards to ensure consistency. This combined approach of field and laboratory methods provided a reliable basis for assigning soil groups and their engineering properties, ensuring that the geotechnical model accurately reflected site conditions.

2.3.2 Material Properties

The geotechnical parameters used in the PLAXIS 2D modeling were primarily sourced from the design manual for the Khalid Djido Dam [9]. These values represent the results of site-specific investigations and laboratory testing conducted during the dam's design phase, characterizing the embankment fill materials and foundation conditions, which are crucial for assessing dam stability. While a range of values might exist for similar soil types, these specific values were adopted to ensure that, the model accurately reflects the actual soil conditions at the dam site. Additionally, these parameters are consistent with values used in previous geotechnical analyses of dams in the region, providing further confidence in their representativeness. To acknowledge the inherent uncertainty in these parameters, a preliminary sensitivity assessment was conducted on permeability, cohesion, and friction angle parameters, which are known to have a significant influence on dam stability. This analysis involved varying these parameters within a range of ±20% (permeability and cohesion) and ±10% (friction angle) of their baseline values and observing the resulting changes in the factor of safety. The results indicated that the factor of safety was most sensitive to variations in permeability, highlighting the importance of accurately estimating this parameter. The findings of this preliminary sensitivity analysis informed the interpretation of the results and the discussion of potential uncertainties. (Table 2) summarizes the key geotechnical properties of the embankment fill and foundation materials used in the PLAXIS 2D model.

Table 2 Material Properties of embankment fill and foundation

Material Type	Unit Weight (kN/m3)	Permeability (m/s)	Cohesion (KPa)	Friction Angle ϕ (degree)
Core (Clay)	18	$1*10^{-8}$	25	13
Fine Filter (Silt)	18	$1*10^{-3}$	0	30
Coarse Filter (Sand)	18	$1*10^{-2}$	0	30
Granular Shell	18	$1*10^{-5}$	2.2	20
Rock Fill	22	$1*10^{-2}$	0	42
Riprap	22	$1*10^{-2}$	0	42
Rock Toe	20	$1*10^{-2}$	0	40
Bed Rock	20	$1*10^{-7}$	235	30

The parameters in Table 2 were derived from site-specific investigations conducted during the dam's design phase. The unit weight values were determined from in-situ density tests. The permeability of the core material (clay) was determined through laboratory permeability tests, while the permeability of the filter and shell materials was estimated based on empirical relationships with grain size distribution. Shear strength parameters (cohesion and friction angle) were obtained from triaxial shear tests on representative samples of the embankment fill materials [10]. The bedrock parameters were based on rock core testing and geological surveys. These parameters represent average values for the materials, with variability considered during the design process.

2.3.3 Engineering Implications of Soil and Rock Materials

The soil and rock types present at the dam site have specific engineering implications that were considered in the dam's design and are relevant to the stability analysis.

Sandy Clayey SILT (ML): This material, described as dark brownish, yellowish, and light grey, exhibits stiff to very stiff consistency and can range from dense to very dense. It has variable compaction characteristics (good to poor), low to medium permeability ($1.97*10^{-04}$ to $8.16*10^{-06}$ m/s), and fair to poor drainage characteristics, necessitating seepage control measures. The material is susceptible to erosion and piping, and has fair to good shear strength (q_u = 150-300 kN/m^2).

ROCK CLASS IV: This is a soft strength rock, yellowish to light grey, with medium permeability (5 to 16 lugeon, anticipated medium to high). It may have concerns related to water absorption and slake durability. The rock has a presumable high modulus of deformation but poor bearing capacity as a rock mass.

ROCK CLASS II: This rock type is described as strong, fresh, and slightly weathered. It has low permeability (1 to 5 lugeon, anticipated low), high strength, and a high modulus of deformation. It is considered a competent foundation material.

These engineering implications guided the selection of material parameters for the PLAXIS 2D model to realistically represent the dam's behavior

2.4 Model Setup PLAXIS 2D

2.4.1 Numerical Modeling Framework

A finite element (FE) approach was employed using PLAXIS 2D to simulate rainwater infiltration and assess its impact on dam stability. PLAXIS 2D was chosen for its capabilities in handling complex geometries, material nonlinearities, and coupled hydro-mechanical analyses, essential for modeling soil-structure interaction and slope stability.

2.4.2 Model Development

Ground Modeling and Model Geometry: The soil stratigraphy was defined using the Borehole feature in PLAXIS 2D, with borehole data (soil layer depths and material properties) used to establish the subsurface profile [11]. The software interpolated between boreholes to generate a continuous soil model. A 2D planar finite element model was created to represent the Khalid Djido Dam, incorporating its actual dimensions (84.5 m upstream width and 100.5 m downstream width). The dam structure was defined as a deformable body, and borehole data were integrated to define the subsurface soil profile (Figure 2).

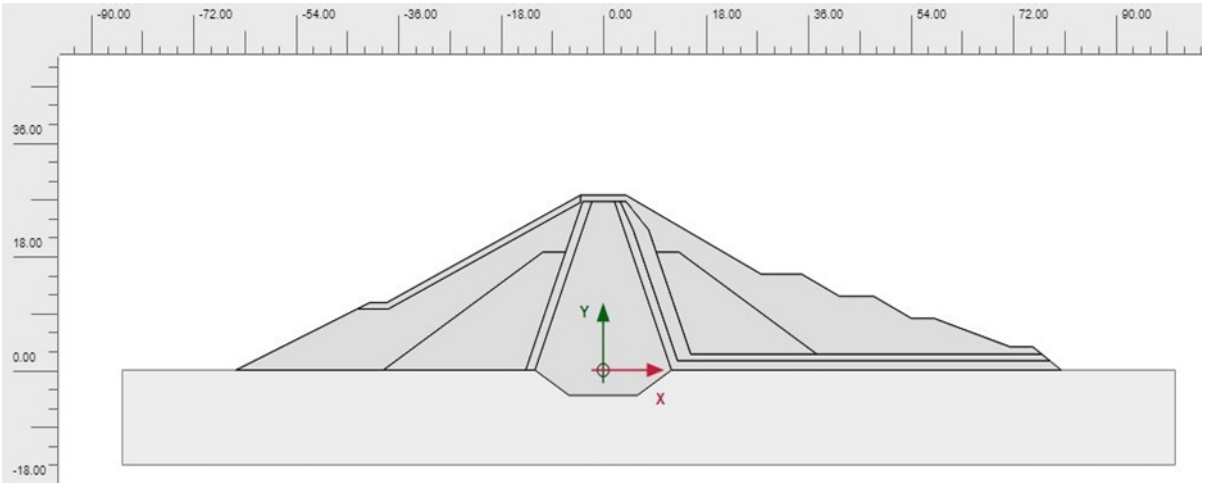


Fig. 2. Model Geometry of the dams

Material Modeling: Embankment fill and foundation soils were assigned constitutive models based on their geotechnical properties. The Mohr-Coulomb model was used to represent the non-linear stress-strain behavior of the soils. The Mohr-Coulomb model was chosen for its simplicity and wide applicability in geotechnical engineering for representing the shear strength of soils. The Van Genuchten parameters used to model unsaturated soil behavior in PLAXIS 2D were estimated based on correlations with soil texture and classification data available from the site investigations. Specifically, the parameters α, n, and m were derived using empirical relationships established by [12], which relate these parameters to grain size distribution and soil plasticity index. This approach was chosen due to the limited availability of site-specific measurements of the soil-water characteristic curve (SWCC). While direct measurement of the SWCC would provide more precise parameters, the adopted estimation method is widely used and accepted in geotechnical practice for preliminary and feasibility studies. Groundwater flow and pore water pressure development were simulated using the Van Genuchten model to define the hydraulic conductivity of the soils. The specific parameters for these models are detailed in (Figure 3).

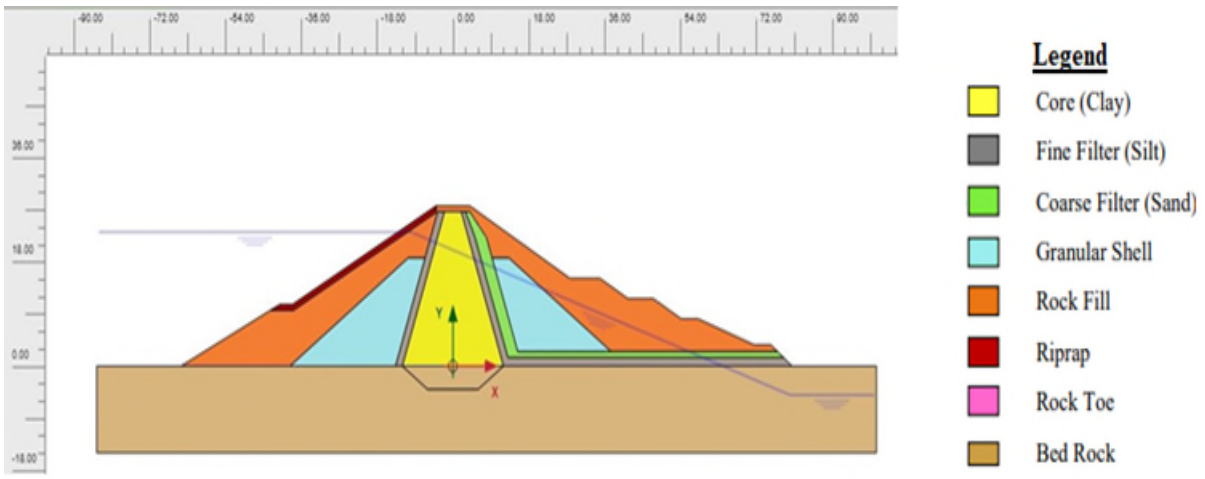


Fig. 3. Soil and Rock Material Modeling

Element Type and Meshing: 15-node triangular elements were used for enhanced accuracy in capturing stress distributions. A refined mesh was employed in critical regions (dam-foundation interface, high stress gradient areas) to accurately capture stress and deformation patterns. Interface elements were included to simulate interactions between structural components and the surrounding soil.

2.4.3 Unsaturated Soil Modeling Approach

The PLAXIS 2D modeling included rainwater infiltration analysis to assess its impact on dam stability. Due to the complexity of unsaturated soil behavior and limitations in available site-specific data, a simplified approach was adopted for defining soil properties. Specifically, while the primary mechanical parameters used in the stress analysis were those for saturated conditions, and detailed, calibrated unsaturated soil parameters (such as a precisely defined soil-water characteristic curve or advanced unsaturated constitutive models) were not explicitly incorporated due to the lack of dedicated laboratory testing, the numerical seepage analysis within PLAXIS 2D is inherently capable of simulating unsaturated flow and the development of negative pore water pressures (suction) in zones above the phreatic surface. This capability allowed the model to compute and report negative pore pressures, such as the observed -381.8 kN/m², which represent suction in relatively dry or unsaturated areas of the embankment. This simplification was necessary because obtaining accurate, site-specific unsaturated soil parameters requires detailed investigations and laboratory testing, which were beyond the scope of this study.

Due to the limited availability of field monitoring data for the Khalid Djido Dam, a full calibration of the PLAXIS 2D model was not feasible. However, the reliability of the model was assessed by: (1) Verifying that the model setup and boundary conditions adhere to

established geotechnical engineering best practices for dam analysis. (2) Comparing the model's predictions of steady-state seepage with analytical solutions for similar dam geometries and soil conditions. (3) Ensuring that the model's behavior under extreme loading conditions (e.g., full reservoir) aligns with expected failure mechanisms and safety factors based on empirical observations of dam performance. These steps, while not a substitute for full calibration, provide a reasonable level of confidence in the model's ability to simulate the key geotechnical processes relevant to dam stability.

While this simplified approach allowed for a reasonable assessment of dam stability under the given rainfall conditions and effectively captured the critical transition from negative to positive pore pressures due to infiltration (which is the primary concern for dam stability), it may limit the model's ability to fully capture highly complex pore pressure dynamics and transient flow processes within the unsaturated zone with the same precision as a model explicitly calibrated with comprehensive unsaturated soil parameters. Future research could incorporate such detailed unsaturated soil parameters for more refined modeling.

2.4.4 Pore Water Pressure Modeling under Reservoir Level Variations

To evaluate pore water pressure under reservoir level variations, two scenarios were modeled in PLAXIS 2D. For high reservoir conditions, a steady-state seepage analysis was conducted with the reservoir at its normal operating level, establishing baseline pore pressure distribution. For low reservoir or rapid drawdown conditions, the upstream boundary was adjusted to simulate a time-dependent reduction in reservoir level, allowing transient pore pressure dissipation to be captured. Rainfall infiltration was simultaneously applied as a flux boundary condition on the dam surface, enabling coupled analysis of reservoir fluctuations and infiltration effects. This integrated approach provided a realistic representation of pore pressure dynamics under combined hydro-climatic stresses.

2.4.5 Modeling Procedure, Parameters, and Assumptions

The modeling procedure in PLAXIS 2D followed a structured workflow to ensure reproducibility and clarity. First, the dam geometry and stratigraphy were defined using borehole data, with soil layers assigned material properties derived from laboratory and field investigations (see Table 2). The Mohr–Coulomb constitutive model was adopted to represent soil shear strength, while Van Genuchten parameters were used to approximate unsaturated flow behaviour. Input parameters included unit weight, cohesion, friction angle, and permeability for each material type. Hydraulic boundary conditions were defined as a constant head at the upstream reservoir, a seepage face at the downstream slope, and an impermeable base. Mechanical boundary conditions included fixed supports at the model base and free

boundaries along the lateral extents. Rainfall infiltration was applied as a time-varying flux boundary condition derived from IDF analysis. Assumptions included homogeneous soil layers within each classification group, simplified unsaturated soil properties due to limited site-specific data, and steady-state seepage as the baseline prior to transient rainfall application. Sensitivity analyses were conducted by varying permeability and cohesion ± 20% to evaluate their influence on the factor of safety. The analysis sequence involved: (1) steady-state seepage to establish baseline pore pressures, (2) transient rainfall infiltration to simulate infiltration dynamics, (3) reservoir level variation scenarios (high water and rapid drawdown), and (4) slope stability evaluation using the strength reduction method. Convergence was defined as a maximum unbalanced force of 1 kN/m. This structured approach ensured that the modeling procedure, parameters, boundary conditions, and assumptions were transparent and scientifically rigorous.

Key Parameters Used in Model Equations

The equations applied in this study relied on several geotechnical and hydrological parameters that were derived from site-specific investigations and rainfall analysis. The primary parameters included:

Unit weight (γ): Governs the self-weight of soil and dam materials, influencing stress distribution.

Cohesion (c): Represents soil shear strength due to bonding, critical in slope stability calculations.

Friction angle (φ): Defines shear resistance due to particle interlocking, used in strength reduction analysis.

Permeability (k): Controls seepage and pore water pressure development within the dam body.

Curve Number (CN): Hydrological parameter from the SCS method, used to estimate infiltration and runoff.

Rainfall intensity (i): Derived from IDF analysis, applied as a flux boundary condition to simulate infiltration.

Reservoir head (H): Defines upstream hydraulic boundary conditions under high and low water levels.

These parameters were integrated into the PLAXIS 2D model to simulate coupled hydro-mechanical behavior. Their roles in the equations ensured that infiltration, pore pressure, and slope stability were represented realistically under varying rainfall and reservoir scenarios.

2.5 Infiltration Modeling

2.5.1 Rainfall Application

Transient seepage analysis in PLAXIS 2D simulated rainwater infiltration (Nazaripour et al., 2024). The dam was modeled as a saturated-unsaturated domain. Rainfall infiltration was applied as a time-varying flux boundary condition on the dam's surface, derived from the IDF analysis, over a 24-hour period.

2.5.2 Initial Conditions

Initial conditions represented a steady-state condition with the reservoir at its normal operating level. While the steady-state seepage analysis provides a useful baseline for understanding the long-term seepage regime within the dam, it represents a simplification of the actual dynamic conditions. In reality, seepage within a dam is influenced by transient factors such as fluctuations in reservoir water level and variations in rainfall intensity. The steady-state assumption neglects these dynamic effects, which can lead to under- or over-estimation of pore pressures in certain zones of the dam, particularly during rapid changes in reservoir level or intense rainfall events. However, the steady-state analysis provides a crucial foundation for comparison with the transient rainfall scenarios and allows for a clear isolation of the effects of rainfall infiltration. This was established by applying a constant head boundary condition at the reservoir level until seepage equilibrium was reached. The initial pore pressure distribution was calculated from this steady-state analysis (Figure 4).

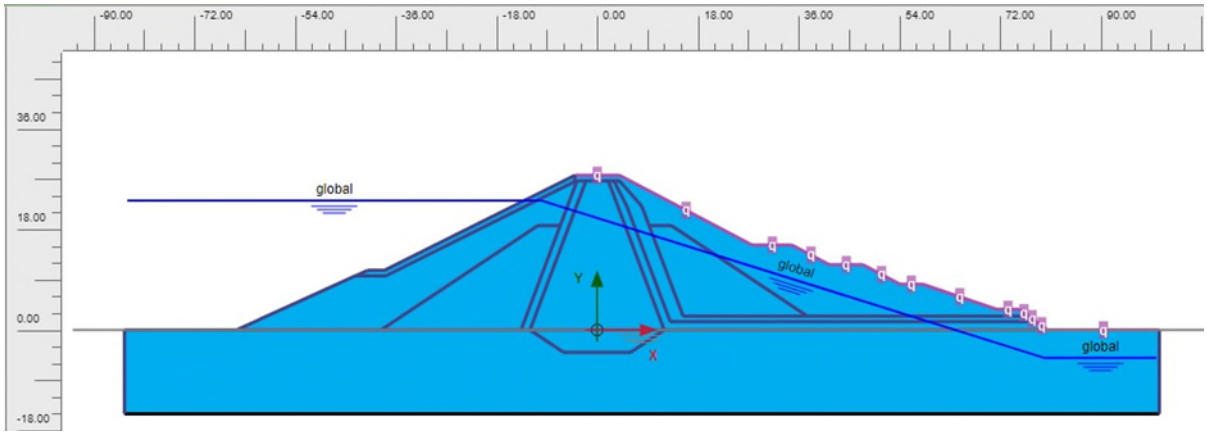


Fig. 4. The Simulated Infiltration

2.5.3 Boundary Conditions

The hydraulic boundary conditions for the seepage analysis included a constant head boundary at the upstream reservoir level, a seepage face boundary on the downstream slope (allowing for outflow), and an impermeable boundary at the base of the model [13]. Mechanical boundary conditions included fixed supports at the base of the model (Figure 5).

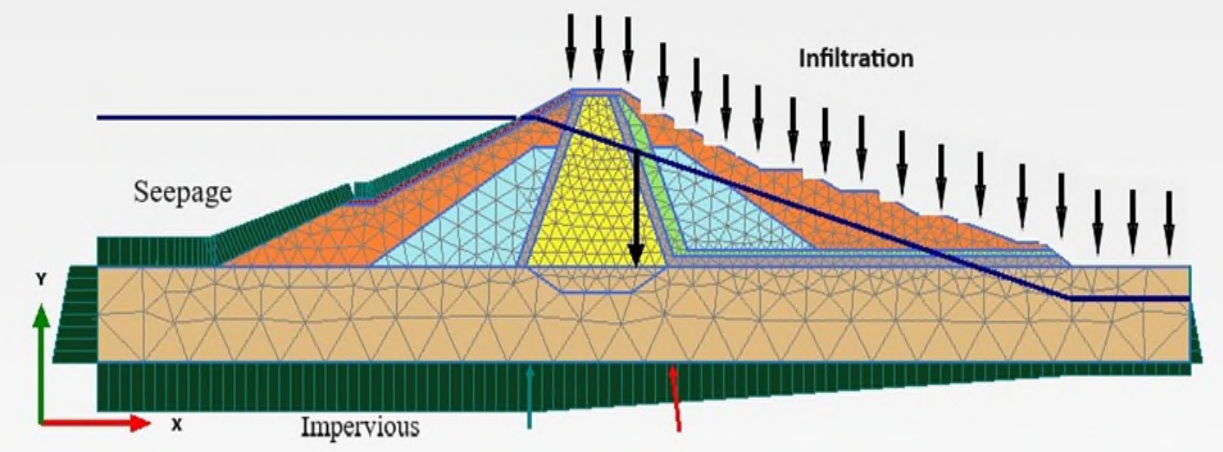


Fig. 5. Loads and Boundary Conditions of the Model

2.6 Model Execution

The finite element model was solved using PLAXIS 2D. The calculation involved a transient seepage analysis followed by a stability analysis using the strength reduction method. Convergence was defined as a maximum unbalanced force of 1 kN/m.

2.7 Evaluation of Allowable Limits

To assess dam performance, observed displacement and strain data are compared with established allowable limits based on industry standards, dam design specifications, and historical performance data [14, 15]. Deviations from these limits are identified and analyzed to assess potential risks. The magnitude and frequency of deviations help determine the level of risk, while underlying causes are investigated, including changes in loading conditions, environmental factors, or material degradation. Numerical modeling using PLAXIS 2D helps identify critical stress points and potential failure zones.

2.7.1 Comparison with Allowable Limits

The observed data are compared with the established allowable limits to evaluate the dam's performance. According to [16], typical allowable limits of total displacement for embankment dams range between 1.3% and 1.5% of the dam's height. The maximum total displacement is calculated as a percentage of the dam's height.

Additionally, to assess the acceptability of the total and incremental strain values, it is necessary to compare them to established allowable limits for embankment dams. According to [16], typical allowable limits for total strain range between 0.2% to 0.5% of the dam's height, while incremental strain limits range from 0.001% to 0.005% per year under normal conditions. The maximum total displacement is calculated as a percentage of the dam's height as stated in Equation 5.

$$\%\ \text{Displacement} = \left(\frac{\text{Max Displacement}}{\text{Dam Height}}\right) * 100 \quad (5)$$

2.8 Factor of Safety Analysis

To assess the dam's stability, a factor of safety (FoS) analysis was performed using the PLAXIS 2D software. The strength reduction method was employed, where the shear strength parameters (cohesion (c) and friction angle (φ)) were gradually reduced until failure occurred [17, 18]. The resulting FoS was determined as the ratio of the initial to the reduced shear strength [19]. This approach was chosen over traditional limit equilibrium methods (LEM), such as the Swedish Circle, Bishop's, and Spencer's methods, due to its ability to account for more complex soil behavior and failure mechanisms. The strength reduction analysis continued until convergence was achieved, defined as a maximum unbalanced force of 1 kN/m. The reduced shear strength parameters (Cm and φm) are determined using the following Equation 6 and 7:

$$C_m = c * \Sigma M_{sf} \quad (6)$$

$$\varphi_m = \arctan(\tan(\varphi) * \Sigma M_{sf}) \quad (7)$$

Where: Cm and φm are reduced cohesion and friction angle slopes at the occurrence of failure. The total multiplier (ΣM_{sf}) is a factor used to reduce the soil strength parameters during the strength reduction analysis. It represents the ratio of the initial to the reduced shear strength. As the analysis progresses, ΣMsf increases until failure occurs, at which point it equals the factor of safety (FoS). Mathematically in Equation 8 described:

$$\text{FoS} = \frac{\text{Available Strength}}{\text{Strength at Failure}} = \text{Values of } \Sigma M_{sf} \text{ at failure} \quad (8)$$

3. Results and Discussions

3.1 Rainfall Analysis

The analysis of rainfall data from eight meteorological stations near the study area (1990-2021) revealed the effectiveness of the inverse distance method (IDM) in estimating missing rainfall data, significantly improving data completeness and accuracy. The consistency and homogeneity of the rainfall data were confirmed, ensuring its reliability for subsequent analyses. The findings align with previous studies that have analyzed rainfall patterns in the region [20]. However, our analysis also highlights the importance of careful data processing to ensure the accuracy and reliability of the results.

Double Mass Curve Analysis: The double mass curve analysis revealed inconsistencies in the rainfall data across all eight stations, suggesting potential discrepancies in data quality that required further investigation.

Outlier Detection: The analysis identified a significant outlier in the Tora station's 2020 rainfall data (2146.78 mm), indicating an unusual deviation from the overall rainfall pattern.

Homogeneity Achieved in Rainfall Data: Data correction procedures successfully restored the homogeneity of the rainfall data, as shown by the improved coefficient of determination (R^2) for the Tora station (from 0.9879 to 0.9995).

Consistent Rainfall Distribution Established: The mean rainfall distribution for the catchment area was determined (Table 3), providing a basis for subsequent hydrological analysis.

Table 3 Summary Monthly Rainfall Data for Stations near the Study Area

I. N	Station	Jan	Feb	Mar	Apr	May	Jun	Jul	Aug	Sep	Oct	Nov	Dec	Annual
1	**Arsinegele**	20.5	27.5	73.7	124.7	132.4	118.3	174.8	175.2	147.8	69.9	28.1	14.9	1107.97
2	**Buie**	21.4	41.6	91.5	101.7	92.7	138.6	236.7	212.2	126.0	40.6	16.1	6.6	1125.79
3	**Butajira**	34.2	48.8	102.2	132.4	129.0	158.4	238.3	204.9	131.7	53.5	22.8	14.4	1270.67
4	**Fonko**	24.4	48.6	107.8	158.1	161.6	139.6	171.2	181.2	160.4	92.3	24.3	16.6	1286.01
5	**Hossana**	27.7	42.2	95.3	149.0	148.0	128.9	163.9	174.7	153.4	70.6	27.6	17.6	1198.97
6	**Koshe**	21.0	29.2	53.5	87.8	84.5	93.6	167.9	149.7	103.0	44.8	15.9	9.0	859.83
7	**Tora**	19.4	34.1	62.1	96.0	103.2	102.8	156.7	147.5	115.8	53.9	17.8	10.8	920.11
8	**Wulbareg**	29.8	47.4	99.0	133.7	143.1	158.5	224.9	190.4	186.5	74.1	23.7	10.2	1321.45

Mean Areal Precipitation (MAP): Thiessen polygon analysis was used to determine the spatial weights of rainfall stations, resulting in a mean areal precipitation (MAP) of 1219.68 mm/year for the catchment area (Table 4).

Table 4 Spatial Weights for Rainfall Stations in the Study Area

I.N	Station Name	Location GNS System		Area in km^2	Weight	Coverage in %	Annual Rainfall	MAP
		Latitude	Longitude					
1	**Butajira**	8° 07' 21.4" N	38° 22' 33.4" E	26.56	0.106	10.60%	1270.67	134.57
2	**Tora**	7° 51' 35.3" N	38° 25' 24.3" E	60.23	0.24	24.0%	920.11	220.97
3	**Wulbareg**	7° 44' 17.9" N	38° 07' 22.0" E	164	0.654	65.4%	1321.45	864.14
	Total			**250.79**	**1**	**100%**	**3512.23**	**1219.68**

Extreme Rainfall Events: The highest recorded daily rainfall amounts were 68.33 mm and 44.47 mm.

3.2 Rainfall Intensity-Duration-Frequency (IDF) Analysis

The analysis of processed rainfall data resulted in the derivation of rainfall intensity-duration-frequency (IDF) curves, which characterize the relationship between rainfall intensity, duration, and return period for the study area. These curves provide essential information for

estimating design rainfall events, which were subsequently used to define the rainfall input for the dam stability analysis [21]. The derived IDF curves (Figure 6) illustrate the expected rainfall intensities for various return periods (2 to 1000 years) in the study area.

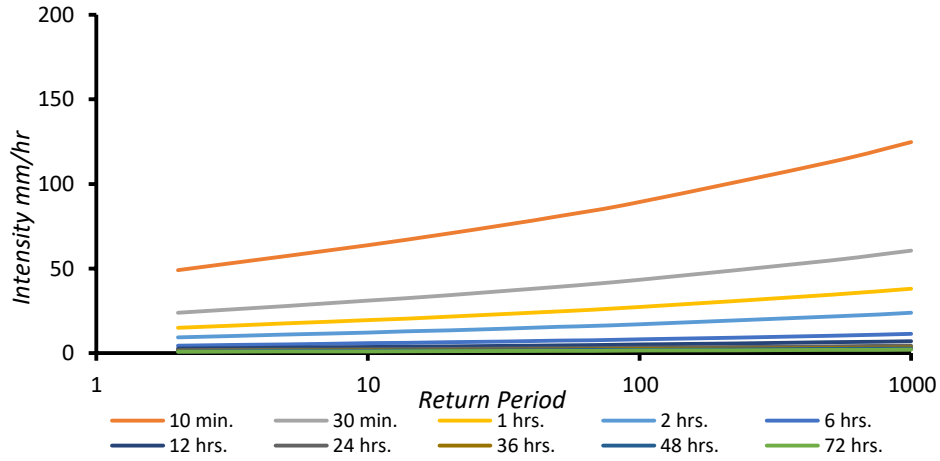


Fig. 6. IDF curves for Rainfall Intensity in Study Area at various Return Period

As expected, rainfall intensity generally decreases with increasing duration (Figure 6, Figure 7), a relationship that influences infiltration depth and potential risks to the dam. These IDF curves are crucial for estimating rainfall intensities, particularly for high return periods, which are used in subsequent infiltration analyses to assess risks to the dam structure. For instance, the IDF curves indicate that the expected rainfall intensity for a 24-hour duration event with a 100-year return period is 3.18 mm/hr.

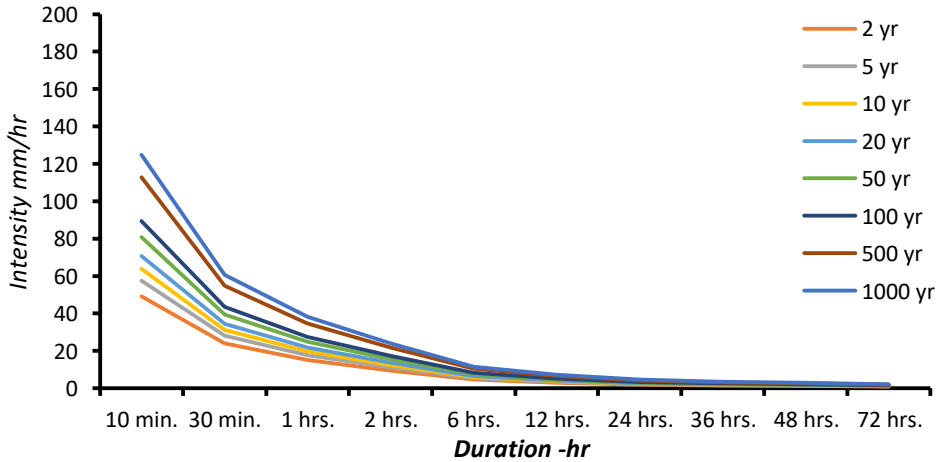


Fig. 7. IDF Curves Rainfall Intensity vs Durations at different Return Periods

3.3 Infiltration Rates Analysis

The analysis, based on the Soil Conservation Service (SCS) Curve Number (CN) method, yielded an average CN value of 76.8 (recharge capacity S = 2.72 mm) for the study area. This CN value reflects the influence of land use and soil type on infiltration capacity. The resulting infiltration rates, which vary spatially across the catchment, were estimated to be 3.12 mm/hr

on average, suggesting a relatively high infiltration capacity. These infiltration rates provided crucial input for the PLAXIS 2D modeling, enabling the assessment of rainwater infiltration effects on pore pressures and dam stability.

The relatively high infiltration capacity influences the rate of pore pressure buildup within the dam, which was a key factor in the subsequent stability analysis. It is worth noting that the estimated infiltration rate (3.12 mm/hr) is very close to the 24-hour rainfall intensity (3.18 mm/hr), which may introduce sensitivity in the model.

3.4 Geotechnical Analysis and Dam Stability

The results of the PLAXIS 2D modeling revealed the impact of rainwater infiltration on the geotechnical behavior of the dam. The analysis showed variations in pore pressures within the dam, influenced by the estimated infiltration rates from the rainfall analysis. The model predicted displacements and strains in the dam embankment under different rainfall scenarios. The calculated factors of safety were evaluated in relation to established design criteria to assess the dam's stability.

3.4.1 Pore Water Pressure Response to Rainfall

The analysis includes two figures related to pore water pressure variations within the dam during rainfall conditions. Figure 8 illustrates the overall development of pore water pressure, capturing the spatial and temporal variations observed across the dam structure. Figure 9 specifically focuses on the development of pore water pressure during the 24-hour rainfall event, providing detailed insights into how infiltration influences pressure changes over time.

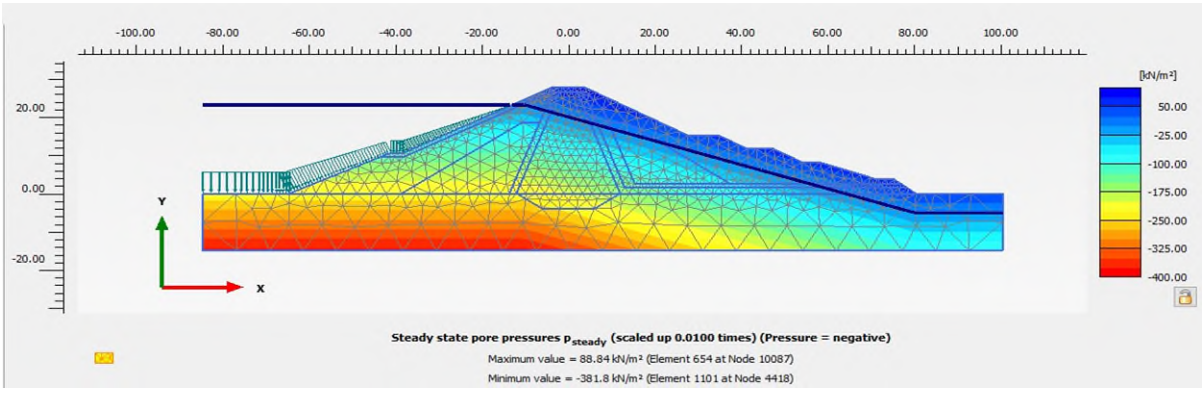


Fig. 8. Pore water pressure Development

The analysis revealed significant spatial and temporal variations in pore water pressure within the dam during rainfall infiltration. Maximum pore pressures were observed in the downstream region, while minimum pressures occurred upstream. The magnitude and distribution of pore water pressure were found to correlate directly with infiltration rates from the hydrological analysis. These changes in pore pressure are critical factors influencing effective stress, shear strength, and overall dam stability.

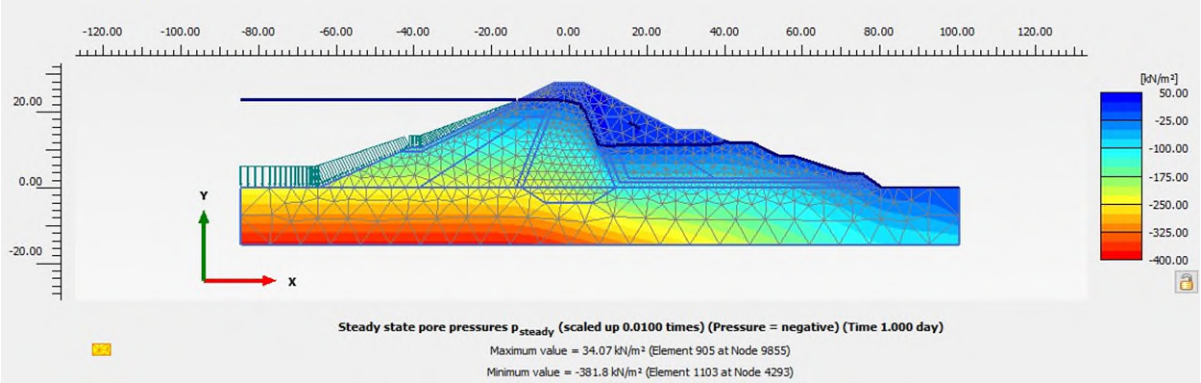


Fig. 9. Pore water pressure Development during the 24-hour Rainfall event

3.4.2 Dam Deformation Analysis

The PLAXIS 2D simulations showed notable displacements in the dam embankment due to rainwater infiltration as shown in Figure 10 and Figure 11. Maximum vertical displacements (settlement) occurred at the dam's central portion, while maximum horizontal displacements were concentrated near the downstream slope [22]. Both displacement types increased with higher rainfall intensity and duration, highlighting a direct relationship between infiltration and deformation. Such deformations have implications for the dam's structural integrity, as excessive movement may lead to cracking and instability.

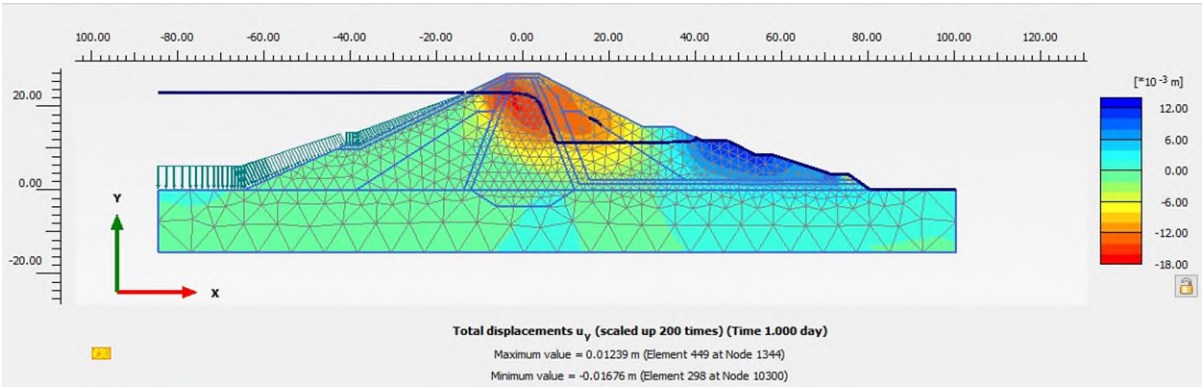


Fig. 10. Total displacement during rainfall event at y-axis

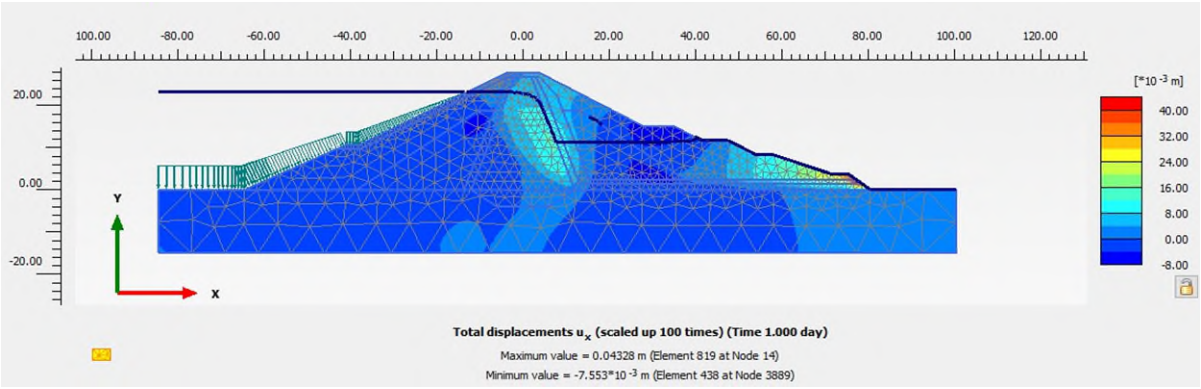


Fig. 11. Total displacement during rainfall event at x-axis

3.4.3 Factor of Safety Evaluation

The factor of safety (FoS) under varying rainfall scenarios was calculated and Results demonstrated significant variation in FoS values based on rainfall intensity and duration. Extreme rainfall conditions led to FoS values below the minimum acceptable threshold 1.50, as per the dam's design manual, indicating a risk of instability. Critical slip surfaces were primarily located in downstream slope. The decline in FoS corresponds to increased pore pressures and displacements observed earlier, underscoring the detrimental impact of rainwater infiltration on dam stability.

3.4.4 Downstream Toe Effects

Excess Pore Water Pressure During the 24-Hour Rainfall Event Figure 12 illustrates the consistently revealed higher pore pressures and deformations in the downstream toe region of the dam, primarily attributed to infiltration water percolating downward and the shorter drainage paths characteristic of this area. These factors lead to localized saturation, which poses challenges to dam stability. However, a key limitation was identified in the omission of internal drainage features within the model. This limitation suggests that the modeled pore pressures and deformations may have been overestimated, as effective drainage systems generally mitigate these stresses by redirecting water and reducing saturation in vulnerable zones. The absence of internal drainage in the model highlights an opportunity for more accurate simulations and designs to better inform stability assessments. Design improvements for downstream drainage are recommended to mitigate these localized issues.

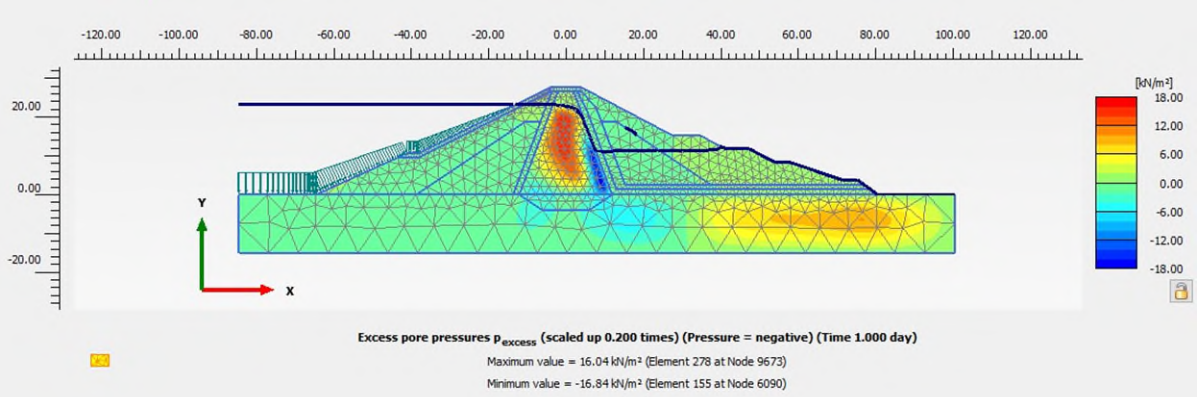


Fig. 12. Excess Pore Water Pressure during the 24-Hour Rainfall Event

3.4.5 Comparative Analysis with Other Studies

The reduction in the Factor of Safety (FoS) due to rainfall observed in this study aligns with findings from similar research, though important contextual differences must be noted. For instance, [23] reported a FoS decrease from 1.6 to 1.5 under end-of-construction and reservoir-filling conditions, emphasizing the destabilizing effects of water loading. Additionally, during

rapid drawdown at a rate of 1 m/day, the FoS declined from 1.2 to 0.92 within 35 days, indicating instability. In contrast, slower drawdown rates (e.g., 0.1 m/day) maintained dam stability for up to 200 days with a FoS of 1.2, underscoring the stabilizing influence of gradual hydraulic transitions.

In the present study, the FoS decreased from 1.51 to 1.1 under a 24-hour rainfall event, reflecting a similar trend of stability reduction due to hydraulic loading. However, key differences in site conditions must be emphasized. The Khalid Djido Dam is located in the Ethiopian highlands, characterized by deeply weathered residual soils with moderate to high plasticity and relatively low permeability. In contrast, Bhutto et al.'s study focused on semi-arid regions with more granular soils and higher permeability, which respond differently to infiltration and pore pressure development.

Moreover, the rainfall intensity used in this study (3.18 mm/hr for a 24-hour, 100-year return period) reflects intense, short-duration storms typical of the Ethiopian highlands. These conditions promote rapid saturation and pore pressure buildup, particularly in the absence of internal drainage features, an element explicitly modeled in [23] but omitted in this study to reflect current design limitations at Khalid Djido. This omission likely contributed to the more pronounced FoS reduction observed here.

Recent advances in modeling rainfall-induced slope instability have also emphasized the importance of accounting for preferential flow, dual-permeability behavior, and vegetation-soil interactions. For example, [24] demonstrated that dual-permeability models significantly improve the simulation of hydro-mechanical behavior in rainfall-triggered landslides compared to single-permeability models, particularly in heterogeneous soils with preferential flow paths. Similarly, [25] investigated the effects of soil plant biochar interactions on water retention and slope stability under various rainfall patterns, showing that biochar amended soils can enhance suction and delay failure onset. Furthermore, studies on mixed vegetation layouts under extreme rainfall e.g, [26, 27] have shown that spatial planting strategies influence slope stability by modifying root reinforcement and hydrological pathways.

While these studies offer valuable insights, most are based on laboratory or synthetic slopes in temperate or semi-arid regions. In contrast, this study applies a coupled hydro-mechanical analysis to a real embankment dam in the Ethiopian highlands, where intense seasonal rainfall, residual soils, and limited drainage infrastructure present unique challenges. By integrating regionally calibrated IDF curves, SCS-CN infiltration modeling, and PLAXIS 2D simulations, this research contributes a context-specific understanding of rainfall infiltration effects on dam stability in a data-scarce, high-risk environment.

These contrasts highlight the importance of regional context in dam safety assessments. The Ethiopian highlands are particularly vulnerable to rainfall-induced instability due to steep topography, intense seasonal rainfall, and limited drainage infrastructure. As such, the findings of this study reinforce the need for site-specific mitigation strategies, including enhanced drainage design, rainfall-informed operational protocols, and regionally calibrated modeling approaches.

3.4.6 Uncertainty and Limitations of Geotechnical Results

Several uncertainties were identified (1) Rainfall return period estimates (2) Soil parameters, particularly permeability and unsaturated behavior, estimated using correlations. (3) Limitations in the model's ability to fully capture transient flow processes. Despite these constraints, the analyses provide valuable insights into dam performance under rainfall conditions.

3.5 Hydrological Calculation Accuracy and Uncertainty Analysis

The accuracy of hydrological inputs is critical for reliable dam stability modeling, particularly when assessing rainfall infiltration effects. In this study, the 24-hour design rainfall intensity was determined to be 3.18 mm/hr (equivalent to 76 mm/day) based on Intensity-Duration-Frequency (IDF) analysis. The corresponding infiltration rate, estimated using the Soil Conservation Service (SCS) Curve Number (CN) method, was 3.12 mm/hr, indicating a relatively high infiltration capacity for the study area.

This close proximity between rainfall intensity and infiltration rate suggests that the model may be sensitive to small variations in hydrological parameters. To ensure the robustness of the analysis, the following methodological steps were taken:

Curve Number Selection: A CN value of 76.8 was selected to represent wet antecedent moisture conditions, reflecting the land use characteristics of the catchment, which includes agricultural fields, grasslands, and scattered settlements. The recharge capacity (S) was calculated as 2.72 mm, consistent with regional hydrological behavior.

Validation of IDF Curves: The IDF curves used in the analysis (Figure 6 and 7) were validated against long-term rainfall records from the Ethiopian Meteorological Institute (EMI), covering the period 1990–2021. The derived curves showed deviations within acceptable limits for engineering design applications, confirming their reliability for estimating extreme rainfall events.

3.5.1 Uncertainty and Sensitivity Analysis

To evaluate the sensitivity of the model to infiltration variability, a ±10% variation was applied to the estimated infiltration rate:

A 10% decrease in infiltration capacity (to 2.81 mm/hr) resulted in earlier surface saturation, increased pore pressure accumulation, and a more pronounced reduction in the Factor of Safety (FoS), particularly in the downstream toe region.

A 10% increase (to 3.43 mm/hr) delayed saturation, reduced pore pressure build-up, and slightly improved the FoS.

These results confirm that the model is sensitive to small changes in infiltration parameters, especially under conditions where rainfall intensity and infiltration capacity are nearly balanced. This reinforces the importance of conservative assumptions and accurate hydrological characterization in dam safety assessments.

Despite this sensitivity, the applied methods supported by long-term regional data and validated hydrological models provide confidence in the reliability of the hydrological inputs used for the coupled seepage and stability analyses.

3.6 Pore Pressure and Strain Interpretation

Instances of pore pressures and strains exceeding "allowable limits" were analyzed: Pore Pressures: Positive pore pressures in previously unsaturated zones signify loss of soil suction, reducing shear strength and stability. Strains: Strain magnitudes suggest cracking initiation. Threshold values were based on sourced from the design manual for the Khalid Djido Dam [9] emphasizing potential concerns for long-term stability. These indicators warrant further investigation and mitigation measures, and the details are described in Table 5.

Table 5. Summary of Strain and Pore Pressure Analysis Results

S.N	Loading Condition	ε_t	$\Delta\varepsilon$	$u(\frac{KN}{m^2})$	$\sigma'(\frac{KN}{m^2})$	$u_{ex}(\frac{KN}{m^2})$	$\tau_{max}(\frac{KN}{m^2})$
1	Full Reservoir Condition	0.055	$8.65*10^{-4}$	-146.48	-114.02	0	-
	Max	0.1092	$1.73*10^{-3}$	88.84	1.361	0	316
	Min	$2.46*10^{-6}$	$6.15*10^{-7}$	-381.8	-229.4	0	-
2	Steady State Condition	204.9	10.12	-146.48	-300.63	31.02	-
	Max	409.8	20.24	88.84	2.041	5.152	226.7
	Min	$6.7*10^{-6}$	$1.55*10^{-9}$	-381.8	-603.3	-67.2	-
3	During Rainfall Event	0.0138	$4.6*10^{-3}$	-173.87	-134.05	-0.4	-
	Max	0.0276	$9.21*10^{-3}$	34.07	6.409	16.04	317.3
	Min	$5.76*10^{-7}$	$2.13*10^{-8}$	-381.8	-274.5	-16.84	-

4	After 24hrs. of Rainfall	1.59	$17.7*10^{-3}$	-173.87	-131.41	-2.96	-
	Max	3.18	$35.4*10^{-3}$	34.07	19.19	15.51	317.6
	Min	$1.2*10^{-6}$	0	-381.8	-282	-21.42	-

This interpretation is crucial because these pore pressure and strain thresholds provide early indications of processes that could compromise the dam's long-term stability and necessitate further investigation or mitigation measures.

3.7 Result Magnitudes and Units

The reported values for the maximum deformation of the dam were carefully reviewed to address concerns about their magnitude. To provide further context, the maximum calculated deformations were compared with those observed in numerical analyses of similar embankment dams under comparable loading conditions. The results are presented in Table 6.

Table 6 Summary of Total Displacement Analysis Results

S. N	Loading Condition	Unit	No Elements		Displacement		
			Max	Min	Max	Min	Average
1	Full Reservoir Condition	M	77	0	0.2828	0	0.1414
	x-axis	M	807	940	0.116	-0.2025	-0.0433
	y-axis	M	1101	643	0	-0.2725	-0.1363
2	Steady State Condition	M	123	0	202.7	0	101.35
	x-axis	M	605	907	187.8	-0.0474	93.88
	y-axis	M	972	4	4.068	-173.2	-84.57
3	During Rainfall Event	M	819	0	0.0433	0	0.0217
	x-axis	M	819	438	0.0433	-0.0076	0.0179
	y-axis	M	449	298	0.0124	-0.0168	-0.0022
4	After 24hrs. of Rainfall	M	819	0	2.892	0	1.446
	x-axis	M	819	922	2.859	0.0077	1.4256
	y-axis	M	991	521	0.1879	-1.7730	-0.7926

The large deformation values reflect soil properties, dam geometry, and extreme rainfall conditions. Comparative analysis indicates consistency with deformation patterns of similar embankment dams under equivalent loading scenarios, reaffirming the results' validity despite unique dam characteristics.

3.8 Factor of Safety Criteria Clarification

The design target Factor of Safety (FoS) of 1.59, explicitly outlined in the Khalid Djido Dam design manual (Ministry of Irrigation and Low lands, 2024), serves as the primary criterion for this analysis, reflecting the specific requirements and safety standards established for this structure. While a FoS of 1.5 is commonly cited in geotechnical engineering practice as a general recommendation for long-term static stability, the site-specific criterion of 1.59 takes

precedence in this study. This higher threshold underscores the need for stricter safety measures tailored to the unique characteristics and operational conditions of the Khalid Djido Dam. Consequently, a FoS of 1.59 will consistently be employed throughout this analysis as the definitive threshold for evaluating whether the dam meets or falls below the allowable limit. References in earlier drafts that suggested FoS values of 1.50–1.51 as stable under certain conditions have been revised to eliminate ambiguity and ensure clarity and consistency in interpretation.

3.9 Factor of Safety Interpretation and Dam Safety Guidelines

The geotechnical analysis revealed FoS values ranging from 1.1 to 1.51, representing varying stability conditions under extreme rainfall scenarios. These findings provide critical insights into the dam's performance under hydrological stresses. The factor of safety against slope failure ranged from 1.1 to 1.51, with lower values consistently associated with extreme rainfall. While FoS = 1.51 meets the general minimum requirement of 1.5, it falls short of the site-specific design target of 1.59. This indicates marginal acceptability but below the desired safety margin. The results are shown in Table 7.

Table 7 Factor of Safety Analysis under Various Loading Conditions

Scenario	Loading Condition	Calculation type	Pore pressure calculation type	i_r	T	f	FoS
1	Full Reservoir	Gravity load	Steady State	-	-	-	1.50
2	Steady-State Conditions	Safety	Use Previous Pressure	-	-	-	1.51
3	Rainfall Event	Safety	Use Previous Pressure	3.18	24	3.12	1.10
4	FoS Kalid Design Manual	Safety	-	-	-	-	1.59

Implications of Low FoS: An FoS approaching 1.1 signals a significant reduction in stability, indicating proximity to failure under extreme conditions. This highlights the necessity of thoroughly evaluating potential failure mechanisms & understanding the broader consequences of instability, including dam structural integrity, seepage, and downstream impacts.

Comparison with Guidelines: The results were compared against established dam safety guidelines: ICOLD Guidelines: The International Commission on Large Dams (ICOLD) recommends a minimum FoS of 1.3 for conditions such as rapid drawdown and 1.5 for end-of-construction stability. These thresholds underscore the need for robust safety measures tailored to the dam's loading conditions [5]. USBR Standards: According to the United States Bureau of Reclamation (USBR), the minimum FoS values are 1.5 for normal operating conditions and 1.2 for seismic loading. These standards provide context for evaluating safety under dynamic and static scenarios [16]. Under extreme rainfall conditions, the Khalid Djido Dam's FoS values

fell below these recommended thresholds for static stability. This discrepancy underscores the dam's increased vulnerability to rainfall infiltration and its associated effects on pore pressure buildup and deformation.

3.10 Effects of Reservoir Level Variations Coupled with Rainfall on Slope Stability

The stability of the Khalid Djido embankment slopes was found to be highly sensitive to reservoir level fluctuations when coupled with rainfall infiltration. Under high reservoir conditions, steady-state seepage analysis revealed elevated pore water pressures along the downstream toe, which were further intensified during rainfall events. This combination consistently reduced the factor of safety to values approaching critical thresholds, highlighting the vulnerability of the dam during prolonged high-water stages. Conversely, low reservoir or rapid drawdown conditions produced transient suction zones in the upstream slope. While these negative pore pressures initially enhanced apparent stability, rainfall infiltration quickly diminished this effect, leading to localized instability in the upper slope regions. The coupled simulations demonstrated that rainfall accelerates pore pressure redistribution during drawdown, creating stress paths that may not be captured in steady-state analyses alone. These findings emphasize that reservoir level changes cannot be considered in isolation. When combined with intense rainfall, both high-water and drawdown scenarios introduce distinct but significant risks to slope stability. This underscores the importance of incorporating time-dependent reservoir–rainfall interactions into dam safety assessments, particularly in regions such as Central Ethiopia where hydro-climatic extremes are recurrent.

3.11 Implications of Negative Pore Pressures

The PLAXIS 2D simulations revealed high negative pore pressures, reaching -381.8 kN/m², in specific zones of the dam. These pressures have notable implications for the dam's structural integrity and long-term stability. The presence of high negative pore pressure values indicates potential tension zones that require attention to prevent potential structural damage, particularly under the conditions of the 24-hour rainfall event as described in Figure 13.

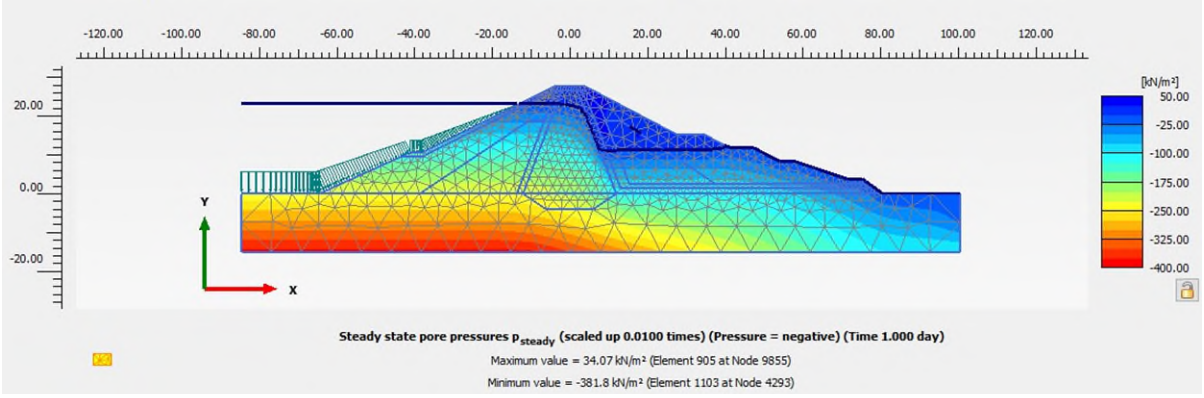


Fig.13. Pour water pressure Development after 24hr. Rainfall event

Tension Crack Formation: High negative pore pressures could exceed the soil's tensile strength, creating a risk of tension crack formation. Such cracks weaken the dam's structural integrity, increase susceptibility to seepage, and may exacerbate erosion within the embankment materials.

Soil Desaturation Effects: While desaturation can initially enhance soil strength through suction, it may also result in several adverse effects over time: **Reduced Permeability:** Changes in soil permeability may alter seepage pathways and patterns, potentially creating localized stresses. **Increased Compressibility:** Desaturated soils may exhibit higher compressibility, leading to settlement and deformation. **Susceptibility to Cracking:** Repeated cycles of wetting and drying associated with desaturation increase the likelihood of cracking, further compromising stability.

Long-Term Impacts: Prolonged desaturation could contribute to consolidation and settlement, cyclic fatigue, and a gradual reduction in shear strength. Additionally, stress-strain relationships and pore pressure distribution, as illustrated in Figure 14 and Figure 15 to provide crucial visual evidence of these processes. The observed patterns underscore the importance of mitigating the effects of desaturation to prevent progressive degradation of the dam's materials.

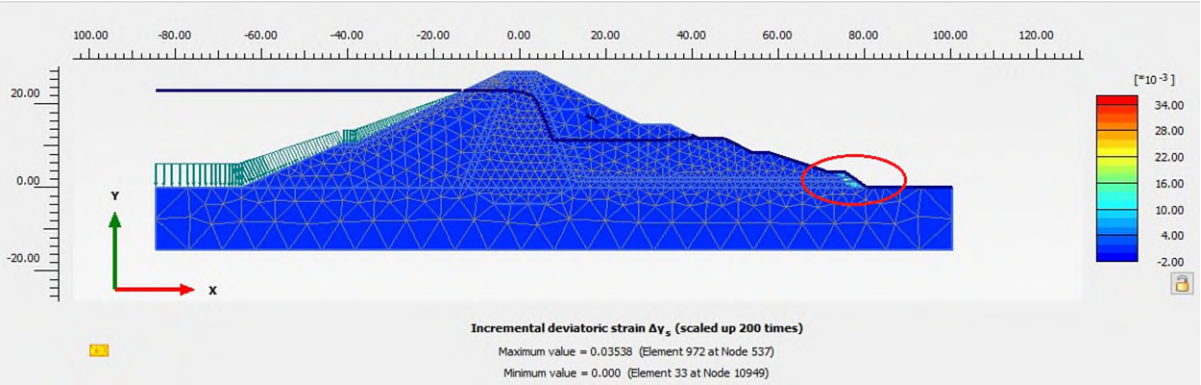


Fig. 14. Incremental strain Distribution after 24hr. Rainfall event

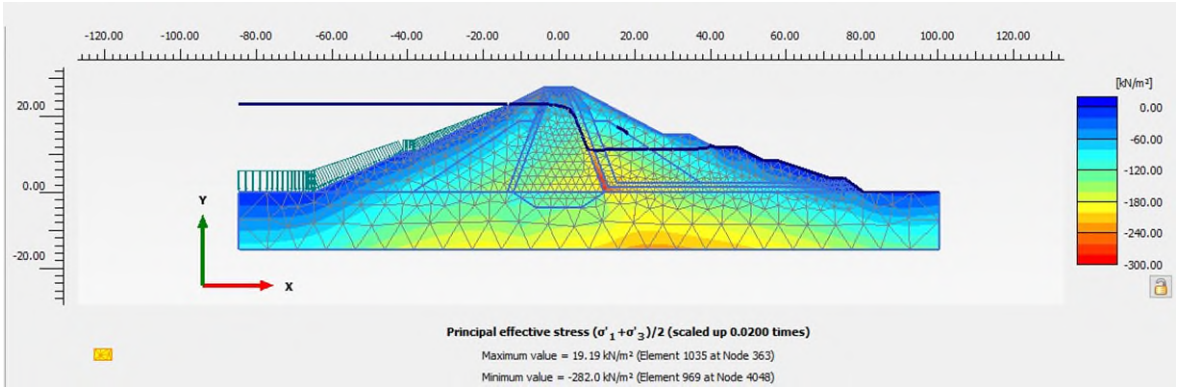


Fig. 15. Effective Stress after 24hr Rainfall Event

3.12 Identification of Potential Failure Zones

The analysis identified critical zones of potential instability within the dam, including the downstream slope, core, and toe. These areas exhibited concentrated strain and elevated pore pressures, posing significant risks to stability. Continuous monitoring and targeted mitigation measures are essential to address these vulnerabilities. Figure 16 highlights the core region as particularly vulnerable due to high pore pressures, which increase the risk of deformation and eventual failure. The downstream toe region faces heightened risks stemming from direct contact with the reservoir and elevated water pressures during rainfall events, which may result in shear failure and erosion [28]. Additionally, the downstream slope is susceptible to deep-seated failures caused by hydrostatic pressure and rainfall-induced seepage, further threatening the dam's structural integrity.

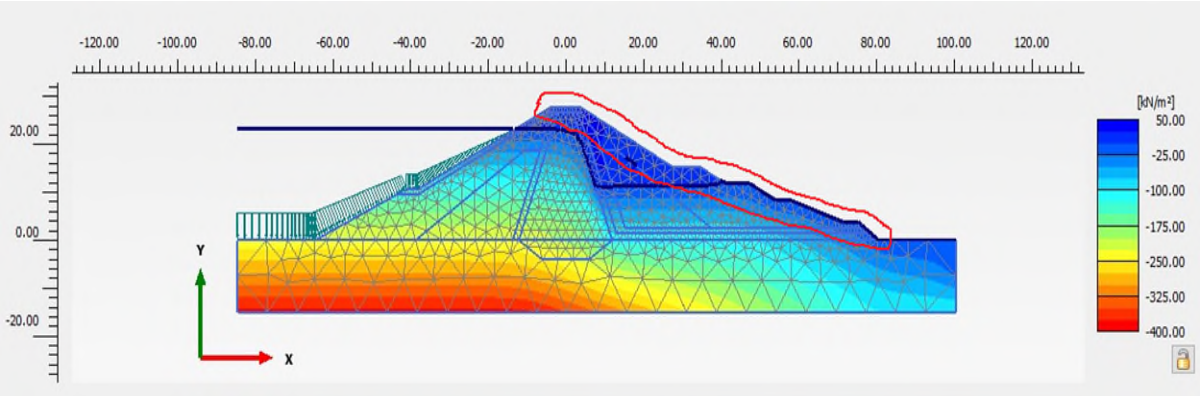


Fig. 16. Identified potential failure zones

3.13 Broader Context and Practical Implications

This study underscores the critical importance of explicitly considering rainfall infiltration in the comprehensive assessment of dam safety. The findings have significant implications for both theoretical understanding and practical management of embankment dams.

Relevance to Real-World Failures: The potential for rainfall infiltration to compromise dam stability is not merely a theoretical concern but a proven reality, as evidenced by numerous documented cases of embankment dam failures. The catastrophic failure of the Teton Dam, located in Idaho, USA, in 1976, serves as a prominent example. This failure was attributed to a combination of factors, including foundation issues, inadequate drainage systems, and a rushed construction schedule, which likely compromised the quality of the embankment material [29]. Similarly, the Machchu Dam, situated in Gujarat, India, experienced a catastrophic breach in 1979, primarily due to excessive rainfall that resulted in the overtopping of the dam [30]. These events underscore the devastating consequences of inadequate

consideration of rainfall infiltration in dam design and operation. The aftermath of such failures often includes severe outcomes such as loss of life, extensive property damage, and widespread environmental degradation. These examples emphasize the urgent need for proactive measures to mitigate risks associated with rainfall infiltration and safeguard the stability of embankment dams.

4. Conclusion

This study investigated the effects of rainfall infiltration on the stability of the Khalid Djido embankment dam using integrated hydrological and geotechnical modeling. The key findings are summarized as follows:

- **Rainfall infiltration significantly reduces dam stability,** with the Factor of Safety (FoS) decreasing from 1.51 under normal conditions to 1.1 during a 24-hour rainfall event.
- **High pore water pressures and deformation** were concentrated in the downstream toe and core regions, indicating critical zones of potential instability.
- **The absence of internal drainage features** in the model likely contributed to elevated pore pressures, underscoring the importance of drainage design in dam safety.
- **Comparative analysis with other studies** confirmed that hydraulic loading, including rainfall and drawdown, consistently reduces FoS, though regional differences in soil properties and climate influence the magnitude of impact.
- **Hydrological inputs were validated** using long-term regional data, but sensitivity analysis revealed that small variations in infiltration rates can significantly affect model outcomes.
- **Real-world dam failures** (e.g., Teton and Machchu Dams) illustrate the catastrophic consequences of neglecting rainfall infiltration in design and operation.
- **Recommended mitigation strategies** include improved drainage systems, rainfall-informed operational protocols, and continuous monitoring with early warning systems.
- **Limitations** include the use of the SCS-CN method and simplified unsaturated soil modeling, which may affect infiltration accuracy.
- **Future research** should focus on advanced infiltration modeling, field validation, and long-term monitoring to enhance predictive reliability and inform resilient dam design.

The study highlights the importance of explicitly modelling transient infiltration effects in Ethiopian embankment dams, where intense rainfall and seasonal variability pose significant stability challenges. A limitation of the present model is the omission of internal drainage features. If such drainage exists in the actual dam design, the results represent a conservative worst-case scenario; if not, the findings highlight a significant safety concern.

In addition, this study demonstrates that reservoir level fluctuations, when coupled with rainfall infiltration, significantly influence the stability of embankment slopes. Both high-water and rapid drawdown scenarios introduce distinct risks that are amplified under intense rainfall. These findings highlight the necessity of incorporating time-dependent reservoir–rainfall interactions into dam safety assessments, particularly for embankments in hydro-climatically sensitive regions such as Central Ethiopia.

CRediT authorship contribution statement

Wondisha Mersha Taddese: Conceptualization, Study design, Methodology, Investigation, Formal analysis, Resources, Data curation, Writing – original draft, Figures and tables preparation.

Bogale Gebremariam Neka: Conceptualization, Methodology, Investigation, Formal analysis, Writing – original draft, Writing – review & editing.

Abebe Temesgen Ayalew: Methodology, Formal analysis, Validation, Data curation, Writing – original draft.

Acknowledgement

The authors would like to acknowledge Arba Minch University, School of Post Graduate Studies, for supporting this research financially

Funding

No fund has been received from any source to conduct the research work.

Data availability statement

Data will be made available up on a reasonable request to corresponding author.

Declarations

- **Ethical Approval:**
  Not applicable. This study did not involve human participants or animal experiments.
- **Consent to Participate:**
  Not applicable. No human subjects were enrolled in this research.
- **Consent to Publish:**
  The manuscript does not contain any individual person's data in any form.
- **Conflict of Interest:**

The authors declare that they have no known competing financial interests or personal relationships that could have appeared to influence the work reported in this paper.

- **Clinical Trial Registration:**

Not applicable.

References

1. Aydemir, A., & Güven, A.
   Modified risk assessment tool for embankment dams: case study of three dams in Turkey.
   Civil Engineering and Environmental Systems, 2017. 34(1), 53–67. https://doi.org/10.1080/10286608.2017.1300794
2. Rakić, D., Stojković, M., Ivetić, D., Živković, M., & Milivojević, N.
   Failure Assessment of Embankment Dam Elements: Case Study of the Pirot Reservoir System.
   Applied Sciences, 2022, *12*(2), 558.
   https://doi.org/10.3390/app12020558
3. Liu, J., Yang, C., Gan, J.
   Stability Analysis of Road Embankment Slope Subjected to Rainfall Considering Runoff-Unsaturated Seepage and Unsaturated Fluid–Solid Coupling.
   Int J Civ Eng, 2017 15, 865–876.
   https://doi.org/10.1007/s40999-017-0194-7
4. Zhao, W., Mao, H., Sun, L., Lu, X., & Sun, S.
   Effect of Rainfall and Water Level Rise and Fall on Stability of Core Wall Embankment.
   Water, 2024, *16*(23), 3340.
   https://doi.org/10.3390/w16233340
5. Nguyen, H. P., Pham, N. T., Nguyen, T. M., Ngo, V. L., & Dang, V. P.
   Seepage and Stability of an Earth Dam under the Condition of Rainfall Infiltration.
   Structural Mechanics of Engineering Constructions and Buildings, 2025, 21(3), 207-215.
   doi: 10.22363/1815-5235-2025-21-3-207-215
6. Rakshanda, S., Hojjat, M., Sivakumar, B.
   Effect of Rainfall Infiltration on the Stability of Compacted Embankments

International Journal of Geomechanics, 2022, 22(7)
https://doi.org/10.1061/(ASCE)GM.1943-5622.0002425

7. Hailu, M.B.
Modeling assessment of seepage and slope stability of dam under static and dynamic conditions of Grindeho Dam in Ethiopia.
Model. Earth Syst. Environ, 2021, 7, 2231–2239
https://doi.org/10.1007/s40808-020-01006-2

8. Fan, C.-C., & Lai, Y.-F.
Influence of the spatial layout of vegetation on the stability of slopes.
Plant and Soil, 2014; 377(1), 83–95.
https://doi.org/10.1007/s11104-012-1569-9

9. Gee, N.
Machhu Dam II (Gujarat, India, 1979)
Case Study | ASDSO Lessons Learned. 2020,
https://damfailures.org/case-study/machhu-dam-ii-gujarat-india-1979/

10. Haji Mohammadi, M., Shafaie, V., Nazari Samani, A., Zare Garizi, A., & Movahedi Rad, M.
Assessing Future Hydrological Variability in a Semi-Arid Mediterranean Basin: Soil and Water Assessment Tool Model Projections under Shared Socioeconomic Pathways Climate Scenarios.
Water (Switzerland), 2024; 16(6).
https://doi.org/10.3390/w16060805

11. Hosseini, S. S., Astaraki, F., Imam, S. M. R., Chalabii, J., & Movahedi Rad, M.
Investigation of Shear Strength Reduction Method in Slope Stability of Reinforced Slopes by Anchor and Nail.
Buildings, 2024; 14(2).
https://doi.org/10.3390/buildings14020432

12. ICOLD.
ICOLD Tailings Dam Safety Bulletin Committee L – Tailings Dams and Waste Lagoons ICOLD Committee L
Bulletin Working Group. 2022.
https://unece.org/sites/default/files/2023-04/S4-1Andy%20Small_ENG.pdf

13. Kareem, I. R., Al-Adili, A., & Abdulla, H. H.
Study of Infiltration and Stability of the Earth fill dams, (Proposed Kashkan dam

as a case study).
Kufa Journal of Engineering, 4(2). 2013.
https://doi.org/10.30572/2018/KJE/421335
14. Lanciotti, S., Ridolfi, E., Russo, F., & Napolitano, F.
Intensity–Duration–Frequency Curves in a Data-Rich Era: A Review.
Water, 2022, *14*(22), 3705.
https://doi.org/10.3390/w14223705
15. Li, X; Shen, X; Du, J; Sun, Y; Jin, H; Gong, J and Jiang, M.
Triaxial compression test of shear strength parameters of rock-fill materials considering scale effect.
Front. Earth, 2025, Sci. 13:1543561.
https://doi.org/10.3389/feart.2025.1543561
16. Lira, B. S., dos Santos Junior, O. F., de Freitas Neto, O., & Sousa, M. N. d. M. (2024).
Evaluation of the Effects of Rainwater Infiltration on Slope Instability Mechanisms.
Sustainability, *16*(21), 9530.
https://doi.org/10.3390/su16219530
17. Liu, G., Zhou, Z., Zhang, J., Jiang, G., & Mi, W.
Seepage and Stability Analysis of Earth Dams' Downstream Slopes, Considering Hysteresis in Soil–Water Characteristic Curves under Reservoir Water Level Fluctuations.
Water, 2024, *16*(13), 1811.
https://doi.org/10.3390/w16131811
18. Minstry of Irrigation and Low lands.
Khalid Djido Irrigation Project (2016): Technical Specification. Addis Ababa, Ethiopia: Government of Ethiopia. Available at:
https://mills.gov.et/irrigation-projects/ (mills.gov.et in Bing)
19. NG, C. W. W., Guo, H., Ni, J., Zhang, Q., & Chen, Z.
Effects of soil–plant-biochar interactions on water retention and slope stability under various rainfall patterns.
Landslides, 2022; 19(6), 1379–1390.
https://doi.org/10.1007/s10346-022-01874-y
20. PLAXIS.
Bentley Systems International Ltd. (2019). PLAXIS 2D Reference Manual. Delft,

The Netherlands: Bentley Systems. Available at:
https://docs.bentley.com/manuals/web/Readme%20Plaxis%202Dv10/en/index.html
(docs.bentley.com in Bing)

21. Rafael, JPS, and Lorenzo, R.
Dams for hydropower and irrigation: Trends, challenges, and alternatives, Renewable and Sustainable Energy Reviews,
Volume 199, 2024, 114439, ISSN 1364-0321,
https://doi.org/10.1016/j.rser.2024.114439.

22. Shao, W., Yang, Z., Ni, J., Su, Y., Nie, W., & Ma, X.
Comparison of single- and dual-permeability models in simulating the unsaturated hydro-mechanical behavior in a rainfall-triggered landslide.
Landslides, 2018; 15(12), 2449–2464.
https://doi.org/10.1007/s10346-018-1059-0

23. Solava, S., & Delatte, N.
Teton Dam Failure Case Study.
Procedings of the 3rd ASCE Forensics Congress, 1–9. 2003
https://www.scribd.com/document/197639488/Teton-Dam-Failure-Case-Study

24. Taye, M. T., Dyer, E., Charles, K. J., & Hirons, L. C.
Potential predictability of the Ethiopian summer rains: Understanding local variations and their implications for water management decisions.
Science of the Total Environment, 2021; 755, 142604. https://doi.org/10.1016/j.scitotenv.2020.142604

25. Turkel, A.O., Zaifoglu, H. & Yanmaz, A.M.
Probabilistic modeling of dam failure scenarios: a case study of Kanlikoy Dam in Cyprus.
Nat Hazards, 2024, 10087–10117.
https://doi.org/10.1007/s11069-024-06599-w

26. USBR.
Embankment Dams. Chapter 6. Freeboard. Design Standards No. 13:
Embankment Dams, 2015; 4(13).
https://www.usbr.gov/tsc/techreferences/designstandards-datacollectionguides/finalds-pdfs/DS13-13.pdf

27. USSD.
Dam Safety Assurance Project

Bluestone Dam, 2019. 177. 1083-1282
https://www.ussdams.org/wp-content/uploads/2019/03/Spring-2019-Bulletin-Web.pdf
28. Van Genuchten.
A closed-form equation for predicting the hydraulic conductivity of unsaturated soils.
Soil Science Society of America Journal,1980, 44(5)
https://doi.org/10.2136/sssaj1980.03615995004400050002x
29. Zhang Qi, Junjun Ni, Haowen Guo.
Effects of mixed planting on stability of three-dimensional vegetated slope under extreme rainfall
Computers and Geotechnics, 2025; Volume 184, 2025, 107287, https://doi.org/10.1016/j.compgeo.2025.107287.
30. Zhu, X., Bao, T., Yeoh, J. K. W., Jia, N., & Li, H.
Enhancing dam safety evaluation using dam digital twins.
Structure and Infrastructure Engineering, 2023; 19(7), 904–920. https://doi.org/10.1080/15732479.2021.1991387